An Electrically Pre-Equalized 10-Gb/s Duobinary Transmission System

Mohamed M. El Said, *Student Member, IEEE*, John Sitch, *Member, IEEE*, and Mohamed I. Elmasry, *Fellow, IEEE*

***Abstract*—Duobinary signaling is combined with a proposed electrical pre-equalization scheme to extend the reach of 10-Gb/s signals that are transmitted over standard single-mode fiber. The proposed scheme is based on predistorting the duobinary signal using two T/2-spaced finite-impulese response (FIR) filters. The outputs of the FIR filters then modulate two optical carriers that are in phase quadrature. Simulation results show that distances in excess of 400 km at bit-error rates less than 10^{-15} are possible. Incorporating a forward-error correction scheme can extend the reach to distances in excess of 800 km. The reach limitation arises not from chromatic dispersion but from fiber nonlinearity, relative intensity noise due to phase-modulation-to-amplitude-modulation noise conversion, and optical amplifier noise accumulation. To demonstrate the feasibility of implementing the proposed scheme, a test chip is implemented in a 0.5-μm SiGe BiCMOS technology. The chip incorporates two 10-tap T/2-spaced FIR filters, which are sufficient to equalize a 10-Gb/s duobinary signal that is transmitted over distances in excess of 400 km. The pre-equalization capabilities of the chip are tested by postprocessing the measured chip output to mimic the effects of the optical channel.**

***Index Terms*—Chromatic dispersion, duobinary modulation, electrical equalizer, optical communication.**

I. Introduction

CHROMATIC DISPERSION is a major fiber impairment that limits the upgrade of standard single-mode fiber (SSMF) to higher bit rates. This is particularly problematic for systems operating in the 1550-nm band where the chromatic-dispersion limit decreases rapidly in inverse proportion to the square of the bit rate. For example, systems running at 2.5 Gb/s can cover distances of 940 km with only a 1-dB power penalty due to chromatic dispersion, whereas at 10 and 40 Gb/s, the distance shrinks to only 60 and 4 km, respectively [1]. Chromatic dispersion can be effectively compensated for using optical techniques, which is only natural to expect given that chromatic dispersion originates in the optical domain. The most mature technique to compensate for chromatic dispersion is by using dispersion-compensating fibers (DCFs) that have a dispersion characteristic that negates that of the original fiber. However, DCFs are expensive and bulky; for every 80–100 km of SSMF, several kilometers of DCF are required and could cost as much as the fiber for which it provides compensation [2]. Since the DCF is added to compensate for fibers that are already installed, its length does not add to the total length of the link. Instead, the DCF sits at one end of the link on a drum. This adds to the total attenuation of the link (the DCF has a typical attenuation of 0.5 dB/km) so that additional amplification may be needed. Furthermore, the narrow core of a DCF renders it more susceptible to fiber nonlinearity effects. The DCF is also polarization sensitive. On the other hand, electrical equalization can offer the advantages of more flexibility, a lower cost, and a smaller size through integration within the transceiver electronics.

For conventional direct-detection receivers, the linear distortion that is induced by chromatic dispersion in the optical domain is transformed into a nonlinear distortion in the electrical signal, which explains why only limited performance improvements can be achieved by using a linear baseband equalizer with only one baseband received signal. This also explains why nonlinear techniques, such as decision feedback equalization and maximum-likelihood sequence detection, are more effective in combating chromatic dispersion in direct-detection receivers [3]–[6]. On the other hand, in a coherent detection system, chromatic dispersion is linear in the electrical signal at the receiver, which is why fractionally spaced equalizers with "complex coefficients" can achieve a performance that is limited only by the number of taps used within the equalizer [7] (considering chromatic dispersion only). However, in spite of its potential and successful experimental trials, coherent lightwave systems did not reach the commercial stage so far. This is attributed mainly to the success of wavelength-division multiplexing (WDM) technology with the advent of erbium-doped fiber amplifiers (EDFAs). Another reason is the complexity of coherent transmitters and receivers [8].

The detrimental effect of chromatic dispersion in SSMF can also be reduced by using reduced-bandwidth modulation formats such as optical duobinary signals, which can extend the reach of 10-Gb/s systems to distances in excess of 200 km, compared with approximately 80 km for conventional nonreturn-to-zero (NRZ) ON–OFF keying (OOK) [9], [10].

In this paper, optical duobinary signaling is combined with a proposed electrical pre-equalization scheme to extend the reach of a 10-Gb/s system, which utilizes SSMF and operates in the 1550-nm band, to several hundred kilometers without any optical chromatic dispersion compensation. In fact, the system reach is influenced by other fiber impairments other than chromatic dispersion. The proposed scheme is based on exploiting the linearity of a coherent lightwave system to move the equalization process to the transmitter, where the data is still in its uncorrupted form. More specifically, the duobinary signal is pre-equalized using two tunable T/2-spaced finite-impulse response (FIR) filters. The outputs of the FIR filters then modulate

Manuscript received July 14, 2004; revised September 27, 2004.

M. M. El Said and M. I. Elmasry are with the Department of Electrical and Computer Engineering, University of Waterloo, Waterloo, ON N2L 3G1, Canada.

J. Sitch is with Nortel Networks, Ottawa, ON K2H 8E9, Canada.

Digital Object Identifier 10.1109/JLT.2004.838812

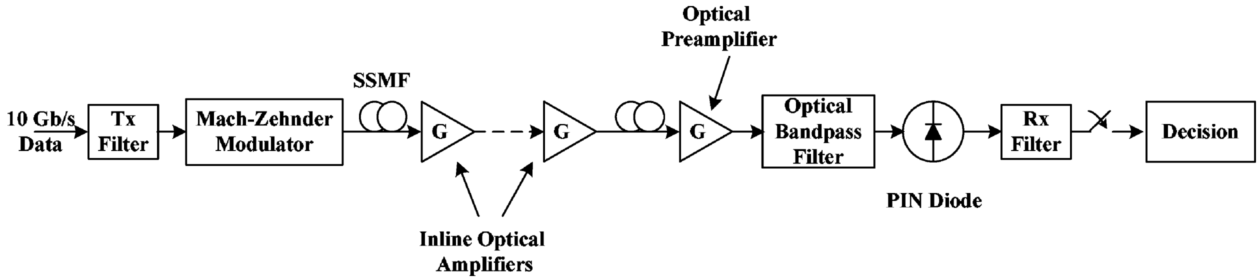

Fig. 1. System overview.

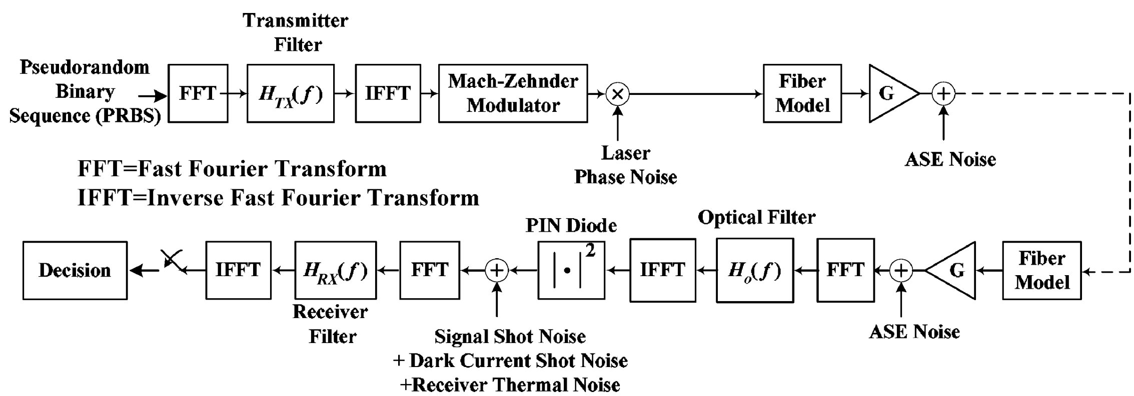

Fig. 2. System model.

two optical carriers that are in phase quadrature. Thus, the advantages of coherent receiver equalization are still maintained while utilizing a conventional noncoherent direct-detection receiver.

Although this paper focuses on duobinary modulation, this choice is principally driven by the reduced-bandwidth advantage, compared with conventional NRZ OOK modulation, and the ability to use a conventional direct-detection receiver. In principle, electrical pre-equalization can also be applied to other modulation formats for potential improvements.

This paper is organized as follows. Section II gives an overview of the considered system. Section III describes the system modeling approach. Duobinary signaling, which is the chosen modulation format, is described in Section IV. The proposed pre-equalization scheme is described in Section V. Simulation results are presented in Section VI. Section VII demonstrates the implementation feasibility of the proposed pre-equalization scheme. Finally, conclusions are given in Section VIII.

II. System Overview

Fig. 1 shows a schematic of the system that is considered in this paper. The system is similar to a typical single-channel point-to-point optical link. The main difference between it and a conventional system is that the transmitted signal is predistorted by a transmitter filter (Tx filter) in order to replace the optical dispersion compensation modules. The transmitter filter also accounts for the limited bandwidth of the transmitter electronics. An external modulator is used to avoid the detrimental effect of chirping that is normally associated with direct laser modulation. More specifically, the modulator is chosen of the Mach–Zehnder type, since its unique characteristics will be exploited to generate the required duobinary signal. Since the proposed scheme extends the reach of the system to several hundred kilometers, inline optical amplifiers are needed to compensate for the link attenuation. The optical amplifiers are assumed to be erbium-doped fiber amplifiers (EDFAs) that have a gain that exactly compensates for the attenuation of each fiber section. An optical bandpass filter is used at the receiver side to limit the noise power detected in the receiver due to the optical amplifiers. The receiver is taken as a conventional receiver, comprised of a p-i-n diode and a low-pass filter which has a bandwidth of approximately 7.5 GHz.

III. System Modeling

The system model is shown in Fig. 2. All system-level simulations are performed using a discrete-time representation of the equivalent complex baseband system. The signals are oversampled at 32 $\times$ the bit rate to mimic the actual continuous-time signals and to avoid spectrum aliasing at any part of the system.

A. Fiber Modeling

To calculate the transfer function of the pre-equalization filter, a linear fiber model is utilized. For system performance evaluation, both a linear and a nonlinear fiber model are utilized.

1) Linear Fiber Model: In the absence of nonlinearities and polarization-mode dispersion, the equivalent baseband transfer function of a fiber of length L can be taken as [11], [12]

$$H_f(f) = e^{-j\left[\left(\frac{1}{2}\right)\beta_2(2\pi f)^2+\left(\frac{1}{6}\right)\beta_3(2\pi f)^3\right]L} \tag{1}$$

where the constant phase terms and the phase terms linear in f are omitted since they do not introduce distortion. β_2, the group-velocity dispersion parameter, is related to the dispersion parameter D through the expression

$$D = -\frac{2\pi c}{\lambda^2}\beta_2 \tag{2}$$

where c is the free-space speed of light and λ is the operating wavelength. β_3, the third-order dispersion, can be related to D and the dispersion slope $S_0 = \partial D/\partial\lambda$ through the relation

$$\beta_3 = \frac{\lambda^2}{(2\pi c)^2}(\lambda^2 S_0 + 2\lambda D). \tag{3}$$

For a non-dispersion-shifted fiber operating in the 1.55-μm band, typically $D \approx 17$ ps/km/nm and $S_0 \approx 0.072$ ps/(km.nm^2). Thus, for a 10-Gb/s signal, we find that $(1/6)\beta_3(2\pi f)^3 \ll (1/2)\beta_2(2\pi f)^2$, and hence the fiber transfer function can be approximately written as

$$H_f(f) = e^{j\xi f^2}, \quad \xi = \pi D\frac{\lambda^2}{c}L. \tag{4}$$

2) Nonlinear Fiber Model: In general, the signal propagation through an optical fiber can be modeled using the nonlinear Schrödinger equation given by [13]

$$\frac{\partial A}{\partial z} + \frac{i}{2}\beta_2\frac{\partial^2 A}{\partial T^2} - \frac{1}{6}\beta_3\frac{\partial^3 A}{\partial T^3} + \frac{\alpha}{2}A = i\gamma|A|^2 A \tag{5}$$

where the nonlinearity coefficient γ is given by

$$\gamma = \frac{n_2\omega_o}{cA_{\text{eff}}} \tag{6}$$

where n_2 is the nonlinear refractive-index coefficient, A_{eff} is the effective fiber area, and ω_o is the light carrier angular frequency. A is a slowly varying pulse envelope (commonly known as the complex envelope) of the passband signal. A is normalized such that $|A|^2$ represents the optical power. α is the fiber loss, and $T = t - z/v_g$ is a frame of reference moving with the pulse at the group velocity v_g. The signal envelope $A(z,t)$ is calculated by solving (5) numerically using the *split-step Fourier method* [13]. A variable step size is implemented according to the nonlinear phase rotation method [14]. The step size is bounded by restricting the maximum nonlinear phase shift per step to 0.01 rad. Reducing the step size any further does not produce significant differences in our results.

B. Noise Modeling

1) Optical Amplifier Noise (Amplified Spontaneous Emission Noise): The amplified spontaneous emission (ASE) noise is modeled as an additive white Gaussian noise (AWGN) in the frequency range of interest. Its one-sided power spectral density in a single polarization is given by [15]

$$N_{\text{ASE}} = N_{\text{sp}}h\nu(G-1) \tag{7}$$

where N_{sp} is the spontaneous emission factor, h is Planck's constant, ν is the optical carrier frequency, and G is the optical amplifier power gain. In the equivalent baseband representation, ASE noise is treated as a complex Gaussian random variable, whose real and imaginary parts are independent and have the two-sided power spectral density $N_{\text{ASE}}/2$ [16], [17]. For simulation, the real and imaginary noise terms are generated such that their variance is

$$\sigma_{I,Q}^2 = \frac{N_{\text{ASE}}}{2}f_s \tag{8}$$

where f_s is the simulator sampling frequency. Noise is then added to the signal after each optical amplifier.

2) Relative Intensity Noise From Phase-Modulation-to-Amplitude-Modulation Noise Conversion: Laser phase noise can be converted to intensity noise by fiber chromatic dispersion (phase-modulation-to-amplitude-modulation (PM–AM) noise conversion occurs), which can result in a significant relative intensity noise (RIN) in the detected optical intensity [18], [19].

Laser phase noise can be assumed to be a Gaussian random process that has a power spectral density $R_\Phi(f)$, given by [19]

$$R_\Phi(f) = \frac{\Delta\nu}{\pi f^2}, \quad 0 < f < \infty \tag{9}$$

where $\Delta\nu$ is the spectral linewidth. The resulting PM–AM RIN was shown in [19] to have a single-sided power spectrum density given by

$$N(f) \approx \frac{1}{2}\left[\sum_{n=0}^{\infty} 4J_n\left(\frac{1}{f}\sqrt{\frac{2\Delta\nu}{\pi}}\right)J_{n+1}\left(\frac{1}{f}\sqrt{\frac{2\Delta\nu}{\pi}}\right) \cdot \sin\left\{\frac{1}{2}(2n+1)(2\pi f)^2\frac{\lambda^2}{2\pi c}DL\right\}\right]^2 \tag{10}$$

where $J_n(x)$ is the Bessel function of the first kind of order n and argument x.

For frequencies above a few hundred kilohertz and source linewidths of a few megahertz, which represents the cases of practical concern, (10) can be simplified to [20]

$$N(f) = \frac{4\Delta\nu}{\pi f^2}\sin^2(4\pi^2 f^2 F_D) \tag{11}$$

where F_D is a dispersion parameter given by

$$F_D = \frac{\lambda^2}{4\pi c}DL. \tag{12}$$

Assuming a receiver with an ideal brick-wall frequency response with bandwidth B_e, the total RIN power within the bandwidth of the receiver can be shown to be [20]

$$\text{RIN}_{\text{PM-AM}} = \frac{2\Delta\upsilon}{\pi B_e}\left[\cos\left(8\pi^2 F_D B_e^2\right) + 4\pi^{\frac{3}{2}}B_e\sqrt{F_D}\,\text{FresnelS}(4B_e\sqrt{\pi F_D}) - 1\right] \tag{13}$$

where FresnelS is the Fresnel sine function.

The laser phase noise is simulated by multiplying the transmitter output by $e^{j\Phi}$, where Φ is a Gaussian random variable that has the power spectral density given by (9).

3) Receiver Shot Noise: The rate of electron-hole generation in the photodiode is modeled as a Poisson process with the parameter $\lambda = P(t).\Re/q$, where $P(t)$ is the instantaneous received optical power, $\Re$ is the photodiode responsivity, and q is the electron charge. A Poisson distribution is defined as

$$p(n) = e^{-\lambda}\frac{\lambda^n}{n!} \tag{14}$$

where n is the rate of electron-hole pairs generation at a certain time, and λ is the average rate of electron-hole pairs generation at that time. The resulting noise is referred to as signal shot noise. Similarly, the dark current shot noise can be modeled as a Poisson process with parameter $\lambda = I_{\text{dark}}/q$, where I_{dark} is the average dark current flowing through the p-i-n diode.

4) Receiver Thermal Noise: Thermal noise is modeled as a white Gaussian random process with a two-sided power spectral density given by

$$S_T(f) = \frac{2KTF}{R_L} \tag{15}$$

where K is the Boltzmann constant, T is the absolute temperature, and R_L is the load resistor in the front end of the receiver. F is the receiver noise figure, which accounts for the excess noise introduced by the various components of the receiver.

C. Mach–Zehnder Modulator Modeling

The transfer characteristic $\psi(t)$ of the Mach–Zehnder modulator (MZM) is modeled by the following equation [20], [21]:

$$\psi\left(v_1(t), v_2(t)\right) = \frac{1}{2}\exp\left(j\pi\frac{v_1(t)}{2V_\pi}\right) + \frac{\gamma}{2}\exp\left(j\pi\frac{v_2(t)}{2V_\pi}\right) \tag{16}$$

where V_π is the MZM's half-wave voltage, $v_1(t)$ and $v_2(t)$ are the voltages applied to the electrodes associated with each arm of the MZM, and the parameter γ accounts for asymmetry between both arms of the MZM. The parameter γ varies within the range $0 \le \gamma \le 1$ and is related to the MZM extinction ratio through the relation

$$\gamma = \frac{\sqrt{\delta} - 1}{\sqrt{\delta} + 1} \tag{17}$$

where δ is the ratio of maximum power to minimum power, measured at the output of the MZM under static conditions. The optical field at the output of the modulator is then given by $E_o\psi(t)$, where E_o is the amplitude of the continuous-wave source input to the MZM.

D. Bit-Error-Rate Simulation

In optical communication, the target BER is typically lower than 10^{-9}, which implies that the time required for Monte Carlo simulations is, practically, not feasible. Instead, quasi-analytical approaches can be used to drastically reduce the simulation time. A common approximation that is employed in the analytical derivations is the Gaussian approximation, in which the probability density function (pdf) of the noise at the receiver is assumed to be Gaussian. Strictly speaking, the pdf of ASE-dominated noise is not Gaussian but is best described by a chi-square distribution [22], [23]. However, the Gaussian approximations can still yield accurate results with only small errors compared with the more accurate methods [24], [25].

Under the assumption of a Gaussian pdf, the probability of error for a one or zero is simply calculated as

$$P_{1,0} = \frac{1}{2}\text{erfc}\left(\frac{|\mu_{1,0} - I_{\text{th}}|}{\sqrt{2}\sigma_{1,0}}\right) \tag{18}$$

where $\mu_{1,0}$ and $\sigma_{1,0}$ are the mean and standard deviation of the one and zero, respectively, and I_{th} is the decision threshold. To take into account the bit pattern effects due to intersymbol interference (ISI), (18) is calculated for every 1 and 0 in the pseudorandom binary sequence (PRBS), and then the BER is simply calculated as the average of all those calculations as shown hereafter [20], [26]:

$$\text{BER} = \frac{1}{2N}\sum_{k=1}^{N}\text{erfc}\left(\frac{|\mu_k - I_{\text{th}}|}{\sqrt{2}\sigma_k}\right) \tag{19}$$

where N is the number of symbols in the PRBS. To obtain the best BER results, it is imperative to adjust the decision threshold for optimum performance. Specifically, the decision threshold has to be lowered toward the logic zero level, since the logic ones are more noisy due to the optical amplification process.

Two approaches are used to calculate the receiver noise variance. The first calculates the receiver noise analytically using the approach outlined in [20] which is based on the theory in [27]. Simulations are just required to get the noise-free waveform at the receiver. Assuming an EDFA preamplifier with a gain G, the variance of the noise current at time τ is expressed as

$$\begin{aligned}\left\langle i^2(\tau)\right\rangle = {} & \Re qG\sum_n P(n\Delta t)h^2(\tau - n\Delta t)\Delta t \\ & + qI_{\text{dark}}\sum_n h^2(n\Delta t)\Delta t \\ & + P_{\text{ASE}}\Re q\sum_n h^2(\tau - n\Delta t)\Delta t \\ & + \frac{(P_{\text{ASE}}\Re)^2}{B_o}\sum_n h^2(\tau - n\Delta t)\Delta t \\ & + \frac{2P_{\text{ASE}}\Re^2 G}{B_o}\sum_n P(n\Delta t)h^2(\tau - n\Delta t)\Delta t \\ & + \frac{2KT_eF}{R_e}\sum_n h^2(n\Delta t)\Delta t + \text{RIN}_{\text{PM-AM}} \\ & \times \frac{(G\Re)^2}{2B_e}\sum_n P^2(n\Delta t)h^2(\tau - n\Delta t)\Delta t\end{aligned} \tag{20}$$

where $\Re$ is the photodiode responsivity, q is the charge of an electron, $P(t)$ is the received optical power before the optical preamplifier, $h(t)$ is the impulse response of the receiver, Δt is the simulation sampling interval, and I_{dark} is the photodiode dark current. P_{ASE} is the ASE noise power in an optical bandwidth B_o due to the inline EDFAs and the EDFA preamplifier. T_e, F, R_e, and B_e are the temperature in Kelvins, noise factor, thermal noise resistance, and noise-equivalent bandwidth of the electrical receiver, respectively. $\text{RIN}_{\text{PM-AM}}$ is given by (13). The noise terms in (20) are identified as signal shot noise, dark current shot noise, shot noise from ASE, spontaneous–spontaneous beat noise, signal–spontaneous beat noise, receiver thermal noise, and RIN, respectively.

The other approach is based on measuring the signal statistics (mean and variance) for each bit in the PRBS sequence from a large number of simulation ensembles and then using them in conjunction with (19) to find the final BER. Compared with an analytical approach, this approach requires much more simulation time. However, the simulation approach can, at times, be more appropriate since it accounts for subtle system effects such as the nonlinear interaction between noise (ASE and laser phase noise on one side) and the optical signal on the other side [28], [29], which are quite difficult to include in the analytical calculations.

Our BER calculations, with their underlying Gaussian approximation, are verified in Section VI-B by Monte Carlo simulations for BERs as low as $\sim 10^{-6}$.

IV. Duobinary Signaling

Duobinary signals belong to the general class of partial-response signals that were first described by Lender [30]. By introducing correlation between successive bits in a binary signal, the signal spectrum can be forced to be more concentrated around the optical carrier. Since chromatic dispersion grows as the square of the frequency, reducing the signal bandwidth helps to increase the reach of the system. A duobinary signal can be obtained by passing the binary antipodal signal through the delay-and-add filter shown in Fig. 3. Assuming the input binary sequence is made up of ideal NRZ pulses with height A and period T, the power spectral density of the duobinary signal is given by

$$S(f) = A^2 T \operatorname{sinc}^2(2fT) \tag{21}$$

which has a power spectral null at a frequency that is equal to half the bit rate ($f = B/2$), as opposed to $f = B$ for an NRZ signal. However, the spectral content of the optical duobinary signal past the $f_c \pm B/2$ band, where f_c is the optical carrier frequency, is still significant enough to offset the gain obtained from the bandwidth reduction. Thus, if a delay-and-add filter is to be used, it becomes imperative to use an analog filter to band-limit the duobinary signal to one half the bit rate in order to obtain an improvement in the dispersion-limited distance [31]. The duobinary filter can also be realized with a low-pass filter having a bandwidth of approximately 25–30% of the bit rate. Bessel filters work particularly well in generating a duobinary signal from an NRZ binary input [20], which makes them the preferred choice for implementation.

In general, duobinary filters generate three-level signals from the input binary stream. Thus, a receiver would normally have to resolve the received three levels and decode them instead of just the two levels of a binary signal, which incurs a sensitivity penalty. However, by exploiting features that are specific to optical links with direct-detection receivers, this sensitivity penalty can be eliminated [32]. The idea is to encode the three levels in both the amplitude and the phase of the optical carrier. If the

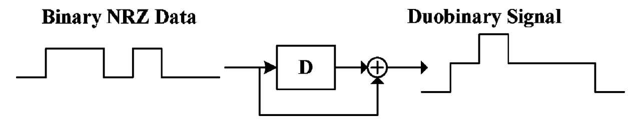

Fig. 3. Digital filter for generating a duobinary signal.

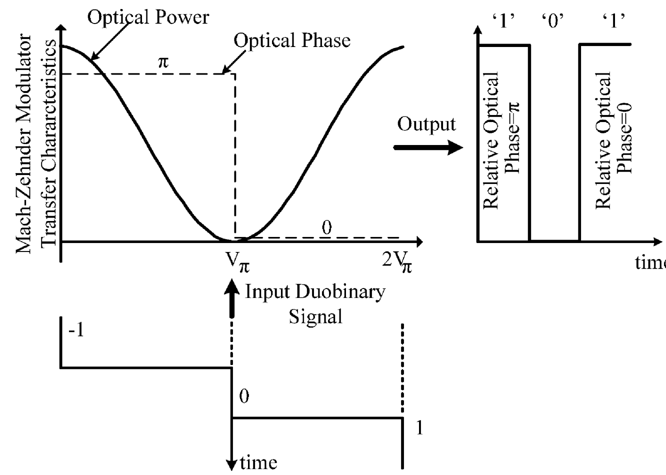

Fig. 4. MZM bias and drive conditions for generating an optical duobinary signal.

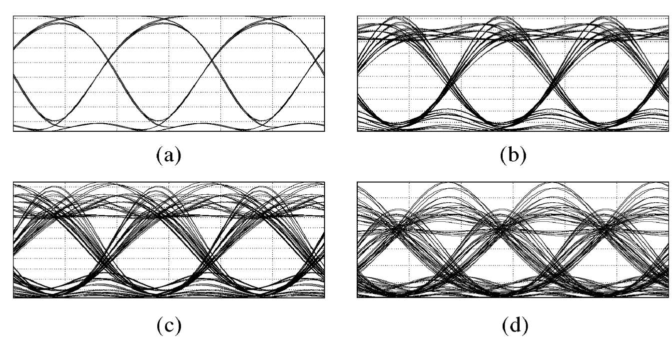

Fig. 5. Simulated receiver eye diagrams for a 10-Gb/s optical duobinary system for different lengths (L) of SSMF. The duobinary signal is generated by a 2.5-GHz fifth-order Bessel filter. (a) $L = 0$ km, (b) $L = 100$ km, (c) $L = 150$ km, and (d) $L = 200$ km.

data is differentially encoded before the duobinary filter,[1] the carrier phase information becomes redundant, and hence, the received data can be decoded using a conventional binary direct-detection receiver. This duobinary signal can be generated by applying a baseband, three-level electrical duobinary signal to a MZM that is biased at maximum extinction, as shown in Fig. 4. Fig. 5 shows an example of a duobinary signal generated by a 2.5-GHz fifth-order Bessel filter.

V. Proposed Pre-Equalization Scheme

In general, chromatic dispersion is a time-varying impairment mainly because of temperature variations [34]. Implications can be quite critical for 40-Gb/s systems that have tight chromatic dispersion tolerances [35]. For example, the range of allowable net dispersion in 40-Gb/s systems is approximately 60 ps/nm. The dispersion in a 40-Gb/s 1000-km link can easily

[1] In general, if binary antipodal data is differentially encoded before being applied to the duobinary filter, then the decoder operates by decoding a 0 level as logic 0 and the levels A and −A as logic 1 [33].

exceed this value (depending on the type of fiber) just by the temperature-induced dispersion variation, even if the accumulated chromatic dispersion is perfectly compensated for at a certain temperature [36]. For 10-Gb/s systems, the chromatic dispersion tolerance is far less stringent than 40-Gb/s systems (approximately 1000 ps/nm for a 1-dB power penalty [1]). Experimental results in [37] showed that the dispersion parameter D in SSMFs operating in the 1550-nm band has a temperature dependence dD/dT approximately equal to -1.5×10^{-3}ps/nm/km/K. This was shown in [38] to cause a variation of approximately 0.15 ps/nm/km in D over the temperature range from -40 °C to 60 °C. Compared with a typical value for D of 17 ps/nm/km, these variations can be neglected. Therefore, it can be assumed, for our immediate purposes, that chromatic dispersion is a static impairment that can be accurately modeled, and hence static equalizers can be utilized.

The ideal zero-forcing equalizer is simply the inverse of the channel transfer function given in (4). Thus, the required equalizer transfer function $H_{\mathrm{eq}}(f)$ is given by

$$H_{\mathrm{eq}}(f) = H_f^{-1}(f) = e^{-j\xi f^2}. \tag{22}$$

However, this transfer function does not maintain conjugate symmetry, that is

$$H_{\mathrm{eq}}(f) \neq H_{\mathrm{eq}}^*(-f). \tag{23}$$

Thus, the impulse response of the equalizing filter is complex. Consequently, this filter cannot be realized by a baseband equalizer using only one baseband received signal, which explains the limited capability of linear equalizers that are used in direct-detection receivers to mitigate the chromatic dispersion. On the other hand, it also explains why fractionally spaced linear equalizers that are used within a coherent receiver can potentially extend the system reach to distances that are only limited by the number of equalizer taps [7]. However, it is important to note that the simulations in [7] did not take into account nonidealities such as the laser phase noise and the fiber nonlinearity, which will eventually set a limit on the maximum achievable transmission distance. Nevertheless, results will be substantially better than those that are achieved by using electrical equalizers in direct detection receivers.

Therefore, instead of building the equalizer in a coherent receiver, most of the complexity can be avoided by building the equalizer at the transmitter, where the data is still in its uncorrupted form. Of course, because the required filter has complex coefficients (from a mathematical point of view), the pre-equalized data have to modulate two optical carriers that are in phase quadrature. Although the concept of using two optical carriers that are in phase quadrature is not a conventional one, its practical feasibility was shown in [39] where two orthogonal optical carriers were used to obtain an optical differential-quadrature phase-shift-keying (oDQPSK) transmission system.

To determine the required equalizer coefficients, the simulation setup in Fig. 6 can be used, where an adaptive algorithm is used to adaptively adjust the FIR filter coefficients to their optimum values. The adaptive algorithm adjusts the FIR filter taps to compensate not only for chromatic dispersion, but also for the inadequacies of the duobinary filter. Once the filter taps converge to their optimal values, the linearity of the system allows transferring the filter to the transmitter side, where it acts as a pre-equalization filter.

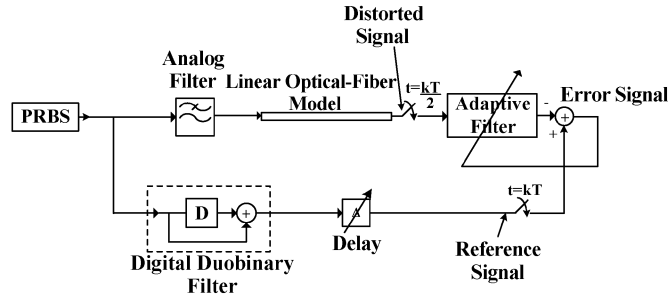

Fig. 6. Simulation setup for determining the pre-equalizer coefficients.

The proposed pre-equalization scheme is depicted in Fig. 7. The optical modulator is composed of a 3-dB optical power splitter, two parallel MZMs, an optical phase shift, and an optical power combiner [39]. The MZMs are biased for minimum optical transmission and driven by the pre-equalized data from the FIR filters. The optical signals from the MZMs are recombined with a relative phase shift of $\pi/2$. The duobinary filters can be implemented either digitally within the FIR filters or using the shown analog filters. In any case, the analog filters also account for the limited bandwidth of the signal path between the pre-equalizer and the MZM electrodes. The tap spacing of the FIR filter can be as high as a whole bit period. However, reducing the tap spacing to half the bit period doubles the frequency band over which equalization can be applied, which translates into a substantial improvement in signal quality, but at the expense of a higher clock speed.

Alternatively, the FIR coefficients can be computed mathematically using, for example, the minimum mean-square-error criterion. This is accomplished by solving the Wiener–Hopf equation, following an approach that is similar to that outlined in [40]. Defining the equalizer tap inputs and tap-weight vectors as (see Fig. 8)

$$\begin{aligned}\mathbf{x}(n) &= [x^*(n) \quad x^*(n-1) \quad \cdots \quad x^*(n-N+1)]^{\mathrm{H}} \\ &= [x(n) \quad x(n-1) \quad \cdots \quad x(n-N+1)]^{\mathrm{T}}\end{aligned} \tag{24}$$

and

$$\begin{aligned}\mathbf{w} &= [w_0 \quad w_1 \quad \cdots \quad w_{N-1}]^{\mathrm{H}} \\ &= [w_0^* \quad w_1^* \quad \cdots \quad w_{N-1}^*]^{\mathrm{T}}\end{aligned} \tag{25}$$

where H denotes the Hermitian transpose. The equalizer output is then expressed in a matrix notation as

$$y(n) = \mathbf{w}^{\mathrm{T}}\mathbf{x}(n). \tag{26}$$

Note that the samples of the equalizer input, $x(n)$, and output, $y(n)$, are at T/2 intervals. However, in the optimization of the equalizer tap weights, only the output samples at T intervals are of concern. Thus, the error signal is defined as

$$e(n) = d(n) - y(2n) \tag{27}$$

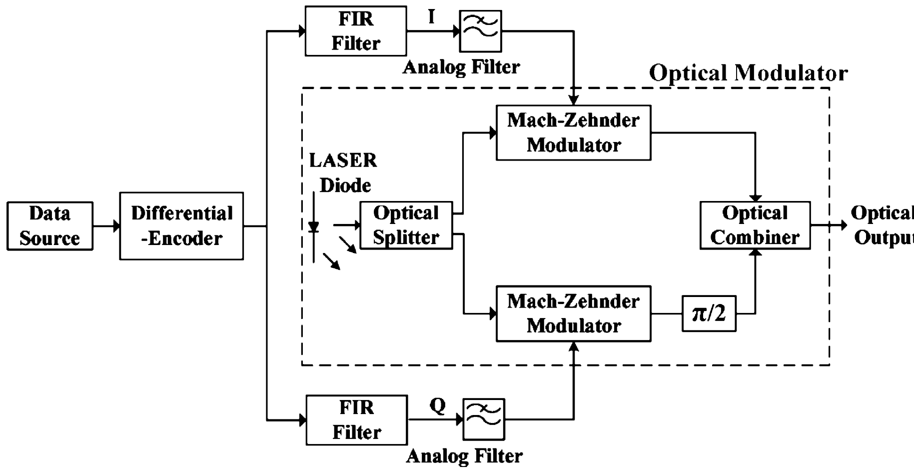

Fig. 7. Proposed pre-equalization scheme.

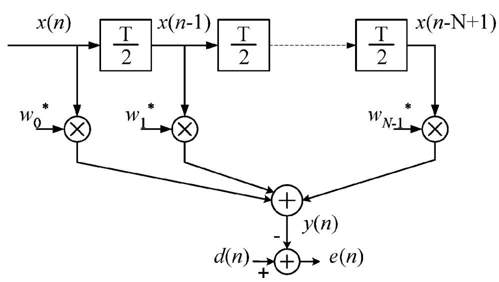

Fig. 8. Fractionally spaced FIR filter.

and thus the performance function to be minimized is written as

$$J = \mathbf{E}\left[e^2(n)\right] \tag{28}$$

where

$$d(n) = \sum_i \gamma_i s(n-i) \tag{29}$$

where γ_i is the impulse response of the digital duobinary filter, padded with enough zeros to account for the delay of the transmitter filter and optical fiber, and $s(n)$ is the uncorrupted data sequence. The fractionally sampled channel response (includes both the transmitter filter and optical fiber) is expressed as

$$\mathbf{h} = [h_0 \quad h_1 \quad \cdots \quad h_{M-1}]^T \tag{30}$$

where M is a sufficiently large integer such that the values of h_i for $i > (M-1)$ are negligible. The optimum tap weights are obtained by solving the Wiener–Hopf equation, which follows from

$$\nabla_{\mathbf{w}} J = 0 \tag{31}$$

which yields the optimum tap-weight vector $\mathbf{w}_0$, given by

$$\mathbf{w}_0 = \mathbf{R}^{-1}\mathbf{p} \tag{32}$$

where

$$\mathbf{R} = \mathbf{E}\left[\mathbf{x}(2n)\mathbf{x}^{\mathrm{H}}(2n)\right] \tag{33}$$

and

$$\mathbf{p} = \mathbf{E}\left[d^*(n)\mathbf{x}(2n)\right]. \tag{34}$$

It can also be shown that

$$\mathbf{x}(2n) = \mathbf{H}\mathbf{s}(n) + \nu(2n) \tag{35}$$

where

$$\mathbf{s}(n) = \left[s(n) \quad s(n-1) \quad \cdots \quad s\left(n - \frac{N}{2} + 1\right)\right]^{\mathrm{T}} \tag{36}$$

$$\mathbf{H} = \begin{bmatrix} h_0 & h_2 & h_4 & h_6 & \ldots & h_{M-2} & 0 & \ldots \\ 0 & h_1 & h_3 & h_5 & \ldots & h_{M-3} & h_{M-1} & \ldots \\ 0 & h_0 & h_2 & h_4 & \ldots & h_{M-4} & h_{M-2} & \ldots \\ \vdots & \vdots & \vdots & \vdots & \vdots & \vdots & \vdots & \vdots \end{bmatrix} \tag{37}$$

and $\nu(2n)$ is a vector of noise samples. The noise, taken to be white noise, is added to avoid excessive filter gains at the frequencies where the magnitude of the channel frequency response is very small. Equation (29) may also be rewritten as

$$d(n) = \gamma^{\mathrm{T}}\mathbf{s}(n) \tag{38}$$

where $\gamma = [0 \ldots 0\,1\,1 \ldots 0]^T$ is a column vector of the target impulse response. Note that the length of γ is appropriately selected by appending extra zeros at its end so that it would be compatible with $\mathbf{s}(n)$. From (33) and (35), and using the fact that $s(n)$ takes the values of 1 and -1 only

$$\begin{aligned}\mathbf{R} &= \mathbf{E}[\mathbf{H}\,\mathbf{s}\,\mathbf{s}^{\mathrm{H}}\,\mathbf{H}^{\mathrm{H}}] + \sigma^2\mathbf{I} \\ &= \mathbf{H}\,\mathbf{I}\,\mathbf{H}^{\mathrm{H}} + \sigma^2\mathbf{I} = \mathbf{H}\,\mathbf{H}^{\mathrm{H}} + \sigma^2\mathbf{I}\end{aligned} \tag{39}$$

where σ^2 is the variance of the added noise, and $\mathbf{I}$ is the identity matrix. Similarly, from (34) and (35)

$$\begin{aligned}\mathbf{p} &= \mathbf{E}[\mathbf{H}\,\mathbf{s}\,\mathbf{s}^{\mathrm{H}}\gamma] \\ &= \mathbf{H}\,\mathbf{I}\,\gamma = \mathbf{H}\,\gamma.\end{aligned} \tag{40}$$

Thus, the desired optimum T/2-spaced FIR equalizer is written as

$$\mathbf{w}_o = \left(\mathbf{H}\mathbf{H}^{\mathrm{H}} + \sigma^2\mathbf{I}\right)^{-1}\mathbf{H}\gamma. \tag{41}$$

TABLE I
SIMULATION PARAMETERS

Parameter	Value
Dispersion parameter, D	17 ps/(nm.km)
Dispersion slope, S	0.072 ps/(nm^2.km)
Laser wavelength, λ	1550 nm
Laser linewidth, $\Delta\nu$	4 MHz
MZM extinction ratio, ER	20 dB
Optical amplifier gain, G	20 dB
ASE factor, N_{sp}	2
Responsivity, $\Re$	0.8 A/W
Nonlinear refractive index coefficient, n_2	2.33e-20 m^2/W
Fiber effective area, A_{eff}	80 μm^2
Fiber attenuation, α	0.25 dB/km
Optical filter bandwidth, B_o	100 GHz
Analog duobinary filter bandwidth	3.5 GHz (3$^{\text{rd}}$ order Bessel filter)

The output of the pre-equalizer is an analog signal that is adversely affected by the nonlinearity of the MZM transfer function. As a result, driving the MZM involves two conflicting requirements. Maximizing the drive voltage reduces the power penalty that results from the MZM's finite extinction ratio, whereas reducing the drive voltage helps to reduce the distortion that results from the nonlinearity of the MZM transfer function. It is found, through simulation, that restricting the maximum input voltage to 70% of the allowable $2V_\pi$ range minimizes the power penalty incurred.[2]

VI. SIMULATION RESULTS

For all the simulation results presented, the pre-equalizer coefficients are obtained by solving the Wiener–Hopf equation as shown in the previous section. Unless stated otherwise, the fiber parameters used for simulation are those listed in Table I.

A. Chromatic Dispersion Compensation Capability

Fig. 9 shows the typical simulated noise-free eye diagrams at the receiver for different fiber lengths. Pre-equalization is performed using two 10-tap T/2-spaced FIR filters. The analog duobinary filter is arbitrarily set to a third-order Bessel filter with a 3-dB bandwidth of 3.5 GHz. The results indicate that 400 km is well within the reach of 10 taps. Beyond 400 km, the quality of the received signal starts to deteriorate, implying that more filter taps are required for pre-equalization.

Fig. 10 shows the effect of increasing the FIR filters' tap spacing, to a whole bit period, on the receiver eye diagrams. Obviously a 10-tap T-spaced equalizer has a larger equalizing time span, and thus, a longer fiber reach is possible. However, the eye diagrams show that for fiber lengths up to 400 km, the quality of the received signal (in terms of jitter and vertical eye opening) is greatly improved by utilizing a T/2-spaced filter.

Fig. 11 shows a plot of the simulated receiver sensitivity versus the fiber length for the conventional NRZ, duobinary,

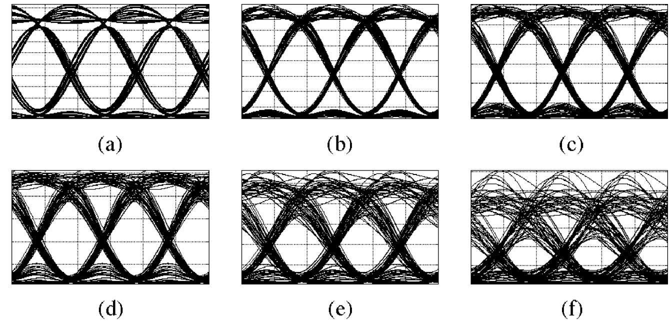

Fig. 9. Simulated receiver eye diagrams of noise-free predistorted 10-Gb/s duobinary data. Pre-equalization is performed using two 10-tap, T/2-spaced FIR filters. (a) $L = 0$ km, (b) $L = 200$ km, (c) $L = 300$ km, (d) $L = 400$ km, (e) $L = 500$ km, and (f) $L = 600$ km.

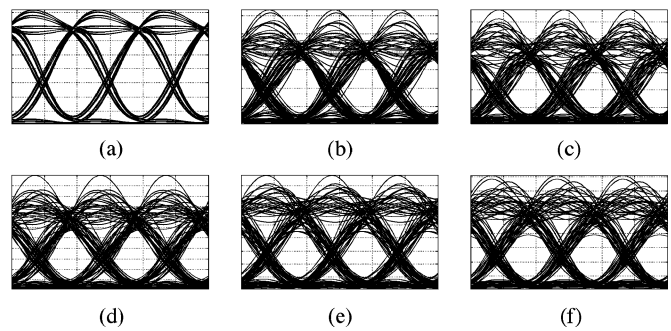

Fig. 10. Simulated receiver eye diagrams of noise-free predistorted 10-Gb/s duobinary data. Pre-equalization is performed using two 10-tap, T-spaced FIR filters. (a) $L = 0$ km, (b) $L = 200$ km, (c) $L = 300$ km, (d) $L = 400$ km, (e) $L = 500$ km, and (f) $L = 600$ km.

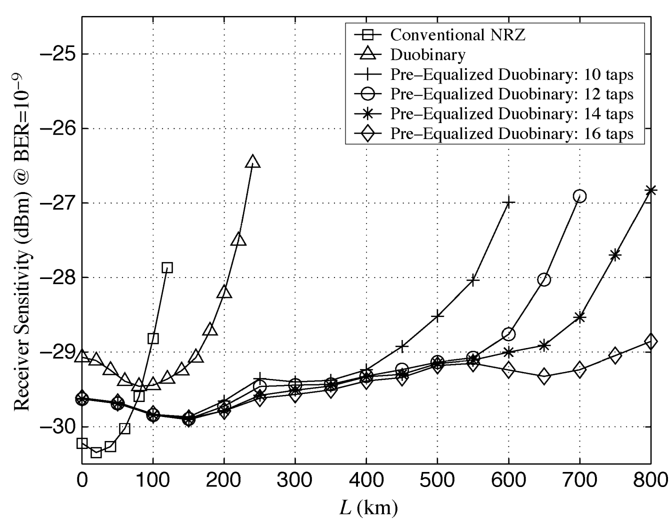

Fig. 11. Receiver sensitivity versus channel length for conventional NRZ, duobinary, and pre-equalized duobinary signals.

and pre-equalized duobinary signals. Only the receiver thermal and shot noise are taken into account. The fiber is assumed to be linear and lossless in order to remove the optical amplifiers from simulations. This serves to isolate the impact of chromatic dispersion at different fiber lengths, thus establishing a common ground for comparing the different modulation schemes. The results show that, given an enough number of pre-equalizer taps, chromatic dispersion can be reduced to acceptable levels for arbitrarily long distances. However, it should be noted

[2]It is possible to eliminate the power penalty due to the MZM nonlinearity by properly predistorting the input signal. This nonlinear signal processing can be achieved by using lookup tables instead of linear FIR filters.

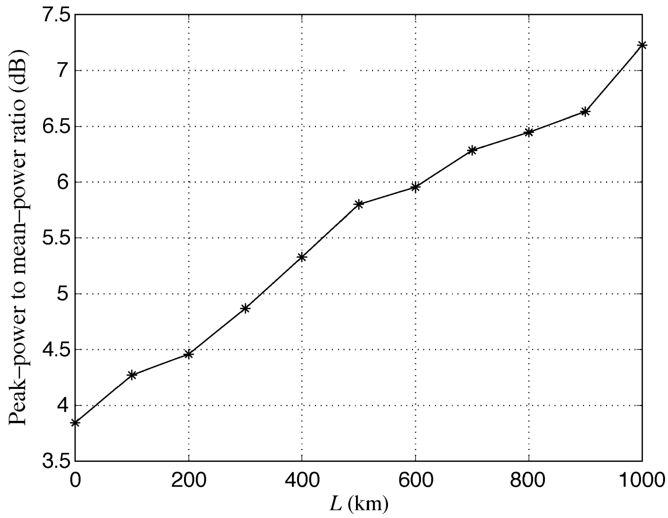

Fig. 12. Transmitter peak-power-to-average-power ratio versus pre-equalized channel length (L) for a 22-tap T/2-spaced pre-equalization filter.

that additional effects such as the nonlinear fiber effects, the accumulation of optical amplifier noise, and the RIN due to the PM–AM noise conversion, become more pronounced as the fiber length is increased, and eventually, limit the capabilities of pre-equalization. One particular side effect of pre-equalization schemes, which is common to all communication channels, is the increase in the peak-power-to-average-power ratio at the transmitter. While conventional NRZ has a peak-power-to-average-power ratio of approximately 3 dB, Fig. 12 shows that increasing the pre-equalized fiber length causes a corresponding steady increase in the peak-power-to-average-power ratio. Since fiber nonlinearities depend on the instantaneous power level, pre-equalization has the negative effect of lowering the maximum allowable average power input to the fiber.

B. Performance of Pre-Equalized 400-, 640-, and 800-km Optical Links

To test the capabilities of the proposed pre-equalization scheme under more realistic transmission impairments, three case studies are considered. Fiber lengths of 400, 640, and 800 km are pre-equalized using 10-, 18-, and 22-tap FIR filters, respectively. The corresponding PRBS lengths are taken as 2^7-1, 2^8-1, and $2^{10}-1$, respectively, which are found to be sufficiently long to include the relevant bit patterns that result in signal distortion. Similar to terrestrial 10-Gb/s systems, running over SSMF and operating in the 1550-nm band, each optical link is divided into 80-km sections. Inline EDFAs of 20-dB gain each are placed between every two sections to exactly compensate for the section attenuation. An optical bandpass filter having a bandwidth of 100 GHz is placed immediately before the receiver p-i-n diode.

Fig. 13 shows the BER curves that are obtained by varying the optical power launched into the fiber. Simulations are performed for various laser linewidths. For comparison, the BER curves are also shown for the three links assuming that ideal optical dispersion compensation modules are inserted every 80 km (i.e., periodic dispersion maps [8]). The results are obtained using a nonlinear fiber model. The noise statistics are measured from 1000 simulation ensembles, and the BERs are calculated from (19). The results demonstrate that effects such as fiber nonlinearity (signal distortion due to self-phase modulation causes the BER curves to bottom out), the RIN due to the PM–AM noise conversion, and the accumulation of optical amplifier noise become more pronounced as the fiber length is increased.

As the link is increased in length, more optical amplifiers are added to compensate for signal attenuation, which has the negative effect of increasing the ASE noise that is accumulated along the link. As a result, the signal power has to be increased to maintain a certain BER. In general, this increase in power does not go unchecked, since it eventually leads to nonlinearity-induced signal distortion that accumulates along the link because of the repeated signal amplification. In the absence of nonlinearity, the total accumulated chromatic dispersion can be compensated at one point along the link without degrading the performance. This is not the case when the nonlinear effects are not negligible. The degradation in the signal quality grows in proportion to the fiber length to the extent that pre-equalization or postequalization, alone, fails to work for the given link setup[3] [8]. Another contributing factor to signal degradation in the considered pre-equalization scheme is the increase in the peak-power-to-average-power ratio, which accelerates the onset of signal distortion.

In the optical domain, the effect of nonlinearity can be effectively reduced by periodically distributing the DCFs along the link such that the total dispersion over each period is close to zero [8]. This way, the signal is periodically corrected before nonlinearity causes significant distortion, thus extending the reach to several thousands of kilometers. This explains why the BER curves of the optically compensated links do not show any sign of degradation within the considered power range. Optically compensated systems are also far less sensitive to PM–AM noise conversion since the average dispersion is kept close to zero.

Despite the aforementioned limitations, the proposed pre-equalization scheme can substantially increase the reach of 10-Gb/s signals running over SSMF. For a 400-km link, the minimum achievable BER (less than 10^{-15}) is low enough so as not to be of any significant practical concern. On the other hand, the 640- and 800-km links are affected by the nonlinearity-induced distortion and the RIN due to the PM–AM noise conversion to the extent that the links become practically unacceptable. A simple and very effective solution is to reduce the transmitted power so as to avoid the nonlinearity problems and use the coding gain of an FEC scheme to make up for the initial increase in BER. Modern FEC schemes can produce BERs below 10^{-15} from raw BERs in the 10^{-3} range at the cost of a few percent overhead. A much more expensive solution, which is commonly used in undersea links, is to reduce the optical amplifier spacing so that the transmitted power per section is reduced, which in turn reduces the nonlinear effects [41].

Finally, to test the validity of the Gaussian approximation that is used for the BER calculations, the results from Monte Carlo simulations[4] are compared to those of the quasi-analytical ap-

[3]This argument holds for both optical and electrical pre-equalization/postequalization.

[4]BER is calculated after detecting at least 100 errors.

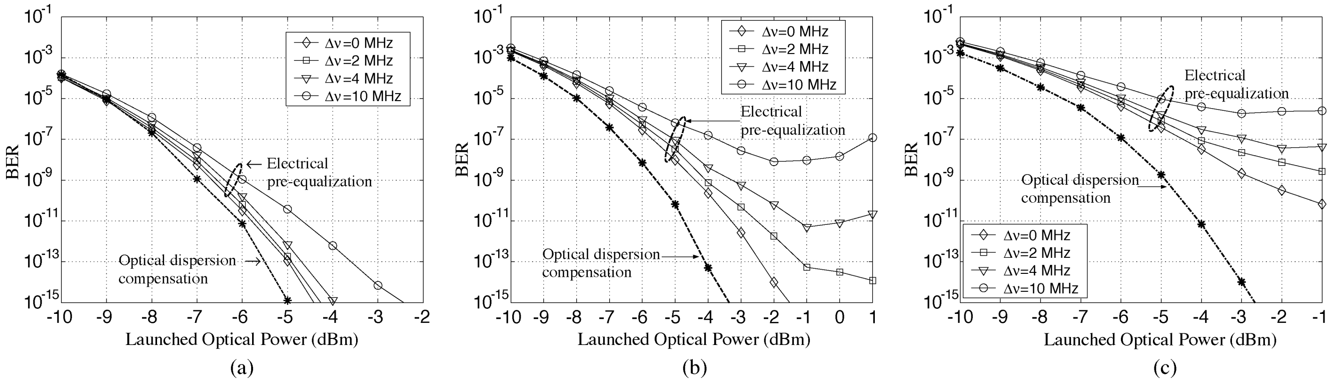

Fig. 13. BER curves for various laser linewidths versus launched optical power. The 400-, 640-, and 800-km links are electrically pre-equalized using 10-, 18-, and 22-tap FIR filters, respectively. The dotted curves are obtained by utilizing ideal optical dispersion compensation modules that are inserted every 80 km along the link. (a) $L = 400$ km, (b) $L = 640$ km, and (c) $L = 800$ km.

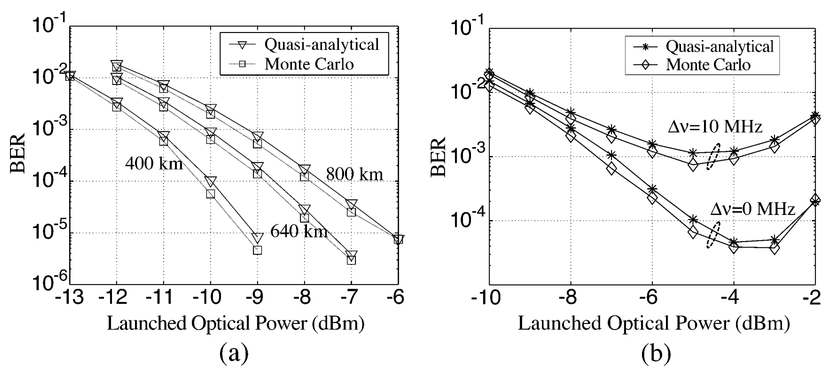

Fig. 14. BER curves obtained by Monte Carlo simulations versus quasi-analytical approach: (a) $L = 400$, 640, and 800 km and $\Delta\nu = 4$ MHz, and (b) $L = 1600$ km.

proach.[5] Fig. 14(a) shows the results for the three fiber lengths that are considered. The BERs are limited to the order of 10^{-6} to keep the simulation times within reasonable limits. To test the approximation under the effect of fiber nonlinearity, an extreme case of 1600 km of fiber is considered, as shown in Fig. 14(b).[6] The results show that the accuracy of the Gaussian approximation is well within the needs of this investigation.

C. Sensitivity to Optical Link Parameters (400-km SSMF Case Study)

Simulation results presented in this section are obtained by utilizing a linear fiber and analytically calculating the noise variance. This simplification allows us to reduce the simulation time substantially. Fig. 15 shows that negligible errors are to be expected around the 10^{-9} BER, which is used to quantify the performance of the system. The receiver sensitivity is calculated by adjusting the received optical power, before the optical preamplifier, until the target BER is obtained.

For calculating the pre-equalization filter coefficients, it is assumed that all the optical link parameters, affecting chromatic dispersion (λ, D, and L) can be accurately measured. Fig. 16(a) and (b) shows the power penalties resulting from the inevitable differences between the actual link parameters

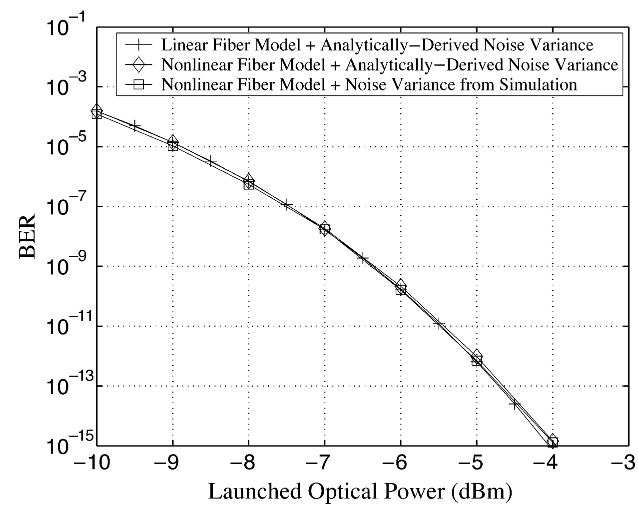

Fig. 15. BER curves obtained by analytically derived and simulation-derived noise variances for linear and nonlinear fiber models ($L = 400$ km and $\Delta\nu = 4$ MHz).

and their nominal/measured values (denoted by the subscript nom) that are used for the design. Since the product of D and L represents the total chromatic dispersion, measured in picoseconds per nanometer, the variations in both D and L can be combined together in one term, as shown in Fig. 16(b). All simulations are performed by varying one parameter at a time, while all other parameters are fixed at their nominal values. Modern measurement equipments can measure these

[5]In this section, the noise variance is measured from simulation.

[6]PRBS length is taken as $2^5 - 1$ to reduce the simulation time. Simulations are only meant to assess the difference between the Monte Carlo approach and the quasi-analytical approach.

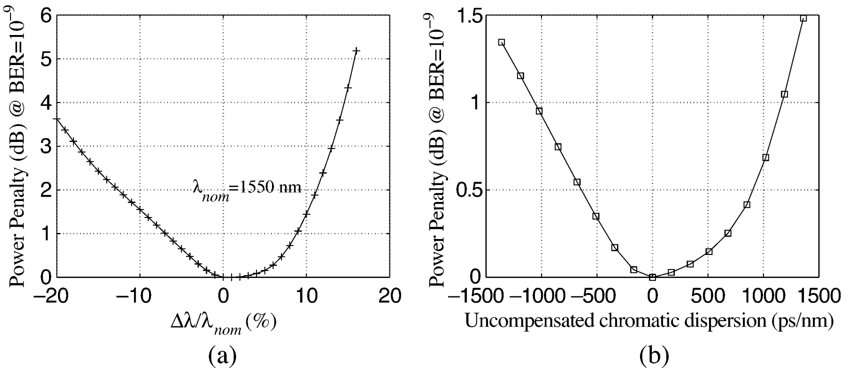

Fig. 16. Power penalty versus: (a) the percentage difference between the actual λ and λ_{nom} and (b) the uncompensated chromatic dispersion.

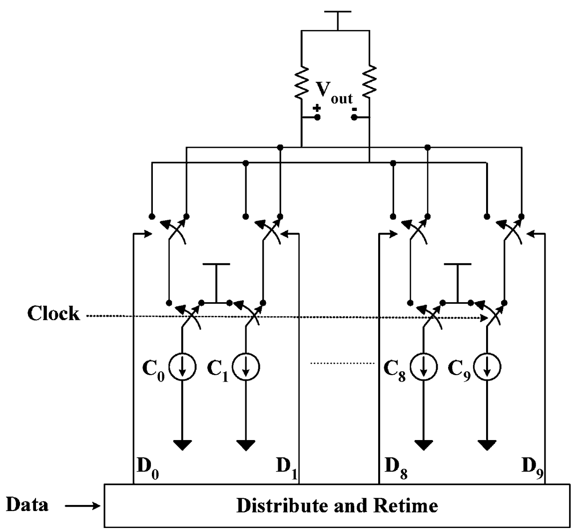

Fig. 17. Simplified schematic of FIR implementation.

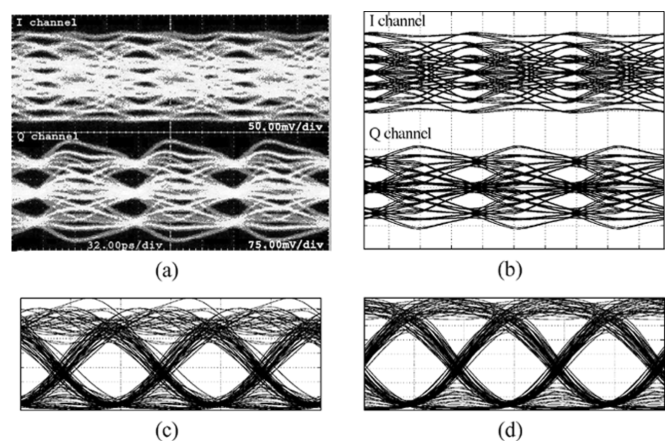

Fig. 18. Eye diagrams for 400 km of SSMF: (a) measured at the chip output, (b) expected chip output from system-level simulations, (c) receiver eye diagram obtained by postprocessing the chip output, and (d) expected signal at the receiver from system-level simulations.

parameters with a high accuracy such that the measurement errors can be considered to be negligible for our purposes. For example, the uncertainty in λ_{nom} is typically less than 0.1 nm, and the uncertainty in D can be kept below $\pm 2\%$. Even if significant measurement errors occur, the somewhat relaxed tolerance suggests that a feedback signal from the receiver to the transmitter can be used to iteratively adjust the transmitter for optimum performance. This adjustment process is required only once for a given link setup.

VII. Implementation Feasibility

To prove the feasibility of implementing the proposed architecture, a test chip is implemented in a 0.5-μm SiGe BiCMOS technology. The chip incorporates two 10-tap, T/2-spaced FIR filters, which are sufficient to equalize a 10-Gb/s duobinary signal that is transmitted over distances in excess of 400 km of SSMF. The filters' coefficients are adjustable using 20 6-b digital-to-analog converters. Fig. 17 depicts a simplified schematic of the chosen FIR implementation. Since the data at the transmitter is in its binary form, data multiplication with the filter coefficients is simply done by switching current sources, representing the magnitudes of the FIR coefficients, to either the positive output or the negative output. The current-source couples $\mathrm{C}_0 - \mathrm{C}_1, \mathrm{C}_2 - \mathrm{C}_3, \ldots\ldots, \mathrm{C}_8 - \mathrm{C}_9$ represent the magnitude of the two samples that are multiplexed within each bit duration. At any instant, only one of each current-source couple is directed toward the output, whereas the other is directed away from the output and drained in the supply. This multiplexing of currents operation is controlled by both the high and low levels of a 10-GHz clock signal to effectively achieve a sampling rate of 20 Gsamples/s.

Fig. 18(a) shows the measured eye diagrams at the outputs of the chip. For comparison, the outputs from system-level simulations are shown in Fig. 18(b). The pre-equalization capability of the chip is tested by postprocessing the measured chip output to mimic the effects of the transmitter, optical fiber, and receiver. The resulting eye diagram at the receiver is shown in Fig. 18(c). Compared with the receiver eye diagram resulting from system-level simulations [shown in Fig. 18(d)], only a small degradation is noticed. This is caused by the relatively high low-cutoff frequencies of the bias-Ts ($\sim$20 MHz) that are used to couple the chip output to the digital sampling oscilloscope input. This increases the jitter of the signals due to the baseline wander effect [33]. This effect is verified by incorporating bias-T models in the system-level simulations. In practice, bias-Ts with a low-frequency cutoff in the kilohertz range are available, which should alleviate this signal degradation. Nevertheless, the overall behavior of the chip is in very good agreement with system-level simulations.

VIII. Conclusion

A proposed pre-equalization scheme is shown to substantially increase the reach of duobinary signals, obviating the need for optical dispersion compensation for distances up to several hundred kilometers. It is shown that, for a 400-km link divided into 80-km spans with EDFAs in between, an error-free transmission (BER better than 10^{-15}) is possible without the help of other dispersion compensation techniques. For longer links, fiber nonlinearity becomes the main limitation, restricting the maximum power that can be launched. An effective solution is to reduce the launched power and use an FEC scheme to lower the BER to acceptable levels. Such an arrangement would enable link lengths in excess of 800 km. For even longer links, combinations of electrical pre-equalization, electrical postequalization, and FEC should result in even larger improvements. The flexibility of electrical pre-equalization can also make it play a complementary role to optical dispersion compensation. Moreover, since the receiver remains unmodified, the postequalization techniques for polarization-mode dispersion are still applicable.

References

[1] "From Loss Test to Fiber Certification Fiber Characterization Today Part I: Chromatic Dispersion," Agilent Technologies, White Paper, Apr. 2003.

[2] J. Ryan, "Fiber considerations for metropolitan networks," *Alcatel Telecommunication Rev.*, pp. 52–55, 1st quarter, 2002.

[3] J. Winters and R. Gitlin, "Electrical signal processing techniques in long-haul fiber-optic systems," *IEEE Trans. Commun.*, vol. 38, no. 9, pp. 1439–1453, Sept. 1990.

[4] F. Buchali, H. Bulöw, W. Baumert, R. Ballentin, and T. Wehreu, "Reduction of the chromatic dispersion penalty at 10 Gbit/s by integrated electronic equalisers," in *Proc. IEEE Optical Fiber Communication Conf. (OFC'00)*, vol. 3, 2000, pp. 268–270.

[5] S. Otte and W. Rosenkranz, "A decision feedback equalizer for dispersion compensation in high speed optical transmission systems," in *Proc. Int. Conf. Transparent Optical Networks*, 1999, pp. 19–22.

[6] C. Fludger, J. Whiteaway, and P. Anslow, "Electronic equalization for low cost 10 Gbit/s directly modulated systems," presented at the Optical Fiber Communication Conf. Exhibit (OFC'04), 2004, p. WM7.

[7] J. Winters, "Equalization in coherent lightwave systems using a fractionally spaced equalizer," *J. Lightw. Technol.*, vol. 8, no. 10, pp. 1487–1491, Oct. 1990.

[8] G. P. Agrawal, *Fiber-Optic Communication Systems*. New York: Wiley, 2002.

[9] W. Kaiser, G. Mohs, T. Wuth, R. Neuhauser, W. Rosenkranz, and C. Glingener, "225 km repeaterless 10 Gb/s transmission over uncompensated SSMF using duobinary modulation and Raman amplification," in *Proc. 14th Annu. Meeting IEEE Lasers Electro-Optics Society (LEOS'01)*, vol. 1, Nov. 2001, pp. 155–156.

[10] M. Wichers, W. Kaiser, T. Wuth, and W. Rosenkranz, "10 Gb/s chirped duobinary transmission (CDBT) over 277 km of uncompensated standard single mode fiber," in *Proc. 4th Int. Conf. Transparent Optical Networks (ICTON'02)*, vol. 1, 2002, pp. 34–37.

[11] E. Forestieri, "Evaluating the error probability in lightwave systems with chromatic dispersion, arbitrary pulse shape and pre- and postdetection filtering," *J. Lightw. Technol.*, vol. 18, no. 11, pp. 1493–1503, Nov. 2000.

[12] G. Keiser, *Optical Fiber Communications*. New York: McGraw-Hill, 2000.

[13] G. P. Agrawal, *Nonlinear Fiber Optics*. San Diego, CA: Academic, 1989.

[14] O. Sinkin, R. Holzlohner, J. Zweck, and C. Menyuk, "Optimization of the split-step Fourier method in modeling optical-fiber communications systems," *J. Lightw. Technol.*, vol. 21, no. 1, pp. 61–68, Jan. 2003.

[15] J. L. Zyskind, J. A. Nagel, and H. D. Kidrof, "Erbium-doped fiber amplifiers for optical communications," in *Optical Fiber Telecommunications IIIB*, I. P. Kaminov and T. L. Koch, Eds. San Diego, CA: Academic, 1997, ch. 9.

[16] D. Marcuse, "Single-channel operation in very long nonlinear fibers with optical amplifiers at zero dispersion," *J. Lightw. Technol.*, vol. 9, no. 3, pp. 356–361, Mar. 1991.

[17] F. Matera and M. Settembre, "Comparison of the performance of optically amplified transmission systems," *J. Lightw. Technol.*, vol. 14, no. 1, pp. 1–12, Jan. 1996.

[18] K. Petermann, "FM-AM noise conversion in dispersive single-mode fiber transmission lines," *Electron. Lett.*, vol. 26, no. 25, pp. 2097–2098, Dec. 1990.

[19] S. Yamamoto, N. Edagawa, H. Taga, Y. Yoshida, and H. Wakabayashi, "Analysis of laser phase noise to intensity noise conversion by chromatic dispersion in intensity modulation and direct detection optical-fiber transmission," *J. Lightw. Technol.*, vol. 8, no. 11, pp. 1716–1722, Nov. 1990.

[20] S. Walklin and J. Conradi, "Multilevel signaling for increasing the reach of 10 Gb/s lightwave systems," *J. Lightw. Technol.*, vol. 17, no. 11, pp. 2235–2248, Nov. 1999.

[21] F. Heismann, S. K. Korotky, and J. J. Veselka, "Lithium niobate integrated optics: selected contemporary devices and system applications," in *Optical Fiber Telecommunications IIIB*, I. P. Kaminov and T. L. Koch, Eds. San Diego, CA: Academic, 1997, ch. 9.

[22] P. A. Humblet and M. Azizoglu, "On the bit error rate of lightwave systems with optical amplifiers," *J. Lightw. Technol.*, vol. 9, no. 11, pp. 1576–1582, Nov. 1991.

[23] Y. Cai, J. M. Morris, T. Adali, and C. R. Menyuk, "On turbo code decoder performance in optical-fiber communication systems with dominating ASE noise," *J. Lightw. Technol.*, vol. 21, no. 3, pp. 727–734, Mar. 2003.

[24] S. L. Danielsen, B. Mikkelsen, T. Durhuus, C. Joergensen, and K. E. Stubkjaer, "Detailed noise statistics for an optically preamplified direct detection receiver," *J. Lightw. Technol.*, vol. 13, no. 5, pp. 977–981, May 1995.

[25] J.-S. Lee and C.-S. Shim, "Bit-error-rate analysis of optically preamplified receivers using an eigenfunction expansion method in optical frequency domain," *J. Lightw. Technol.*, vol. 12, no. 7, pp. 1224–1229, Jul. 1994.

[26] B. K. Whitlock, P. K. Pepeljugoski, D. M. Kuchta, J. D. Crow, and S.-M. Kang, "Computer modeling and simulation of the optoelectronic technology consortium (OETC) optical bus," *IEEE J. Sel. Areas Commun.*, vol. 15, no. 4, pp. 717–730, May 1997.

[27] J. C. Cartledge and A. F. Elrefaie, "Effect of chirping-induced waveform distortion on the performance of direct detection receivers using traveling-wave semiconductor optical preamplifiers," *J. Lightw. Technol.*, vol. 9, no. 2, pp. 209–219, Feb. 1991.

[28] J. P. Gordon and L. F. Mollenauer, "Phase noise in photonic communication systems using linear amplifiers," *Opt. Lett.*, vol. 15, no. 23, pp. 1351–1353, Dec. 1990.

[29] A. V. T. Cartaxo, B. Wedding, and W. Idler, "Influence of fiber nonlinearity on the phase noise to intensity noise conversion in fiber transmission: theoretical and experimental analysis," *J. Lightw. Technol.*, vol. 16, no. 7, pp. 1187–1194, Jul. 1998.

[30] A. Lender, "Correlative digital communication techniques," *IEEE Trans. Commun. Technol.*, vol. COM-12, no. 4, pp. 128–135, Dec. 1964.

[31] S. Walklin and J. Conradi, "On the relationship between chromatic dispersion and transmitter filter response in duobinary optical communication systems," *IEEE Photon. Technol. Lett.*, vol. 9, no. 7, pp. 1005–1007, Jul. 1997.

[32] K. Yonenaga, S. Kuwano, S. Norimatsu, and N. Shibata, "Optical duobinary transmission system with no receiver sensitivity degradation," *Electron. Lett.*, vol. 31, no. 4, pp. 302–304, Feb. 1995.

[33] E. A. Lee and D. G. Messerschmitt, *Digital Communication*, 2nd ed. Norwell, MA: Kluwer Academic, 1994.

[34] W. Hatton and M. Nishimura, "Temperature dependence of chromatic dispersion in single mode fibers," *J. Lightw. Technol.*, vol. 4, no. 10, pp. 1552–1555, Oct. 1986.

[35] M. Yoneyama, Y. Miyamoto, T. Otsuji, A. Hirano, H. Kikuchi, T. Ishibashi, and H. Miyazawa, "Fully electrical 40-Gbit/s TDM system prototype and its application to 160-Gbit/s WDM transmission," in *Proc. Optical Fiber Communication Conf./Int. Conf. Integrated Optics Optical Fiber Communication (OFC/IOOC'99)*, vol. 3, 1999, pp. 128–130.

[36] T. Kato, Y. Koyano, and M. Nishimura, "Temperature dependence of chromatic dispersion in various types of optical fiber," *Opt. Lett.*, vol. 25, no. 16, pp. 1156–1158, Aug. 2000.

[37] M. J. Hamp, J. Wright, M. Hubbard, and B. Brimacombe, "Investigation into the temperature dependence of chromatic dispersion in optical fiber," *IEEE Photon. Technol. Lett.*, vol. 14, no. 11, pp. 1524–1526, Nov. 2002.

[38] P. S. André, A. N. Pinto, and J. L. Pinto, "Effect of temperature on the single mode fibers chromatic dispersion," in *Proc. SBMO/IEEE MTT-S International Microwave Optoelectronics Conf. (IMOC'03)*, vol. 1, 2003, pp. 231–234.
[39] R. A. Griffin and A. C. Carter, "Optical differential quadrature phase-shift key (oDQPSK) for high capacity optical transmission," in *Proc. Optical Fiber Communication Conf. Exhibit (OFC'02)*, 2002, pp. 367–368.
[40] B. Farhang-Boroujeny, *Adaptive Filters Theory and Applications*. New York: Wiley, 1998, ch. 10.
[41] N. S. Bergano, "Undersea amplified lightwave systems design," in *Optical Fiber Telecommunications IIIA*, I. P. Kaminov and T. L. Koch, Eds. San Diego, CA: Academic, 1997, ch. 10.

Mohamed M. El Said (S'97) received the B.Sc. and M.Sc. degrees, both in electrical engineering, from Ain Shams University, Cairo, Egypt, in 1996 and 2000, respectively. He is currently working toward the Ph.D. degree with the University of Waterloo, Waterloo, ON, Canada.

He was a Research Intern with Nortel Networks, Ottawa, ON, Canada, from September 2002 to April 2003, working on the development of electrical equalizers for fiber-optic communications. His current research interests includes equalization for fiber-optic communication systems and high-speed circuit design.

John Sitch (M'03) was born in London, U.K. He received the Engineering Science degree from the University of Oxford, Oxford, U.K., and the M.Eng. and Ph.D. degrees from Sheffield University, Sheffield, U.K., with a thesis on microwave MESFET Mixers and a dissertation on noise in transferred-electron amplifiers.

He formerly worked as a Radio Systems Development Engineer at Plessey Company for two years. For ten years, he taught first at the University of Nottingham, Nottingham, U.K., and then at Sheffield University, with research interests in the areas of semiconductor and electromagnetic device modeling. Since 1984, he has been with Nortel Networks, Ottawa, ON, Canada, working on various aspects of III–V integrated circuits and optical systems, where he is currently advisor on next-generation photonic systems.

Dr. Sitch is the recipient of the R&D100 award in 1996. he was the Chairperson of the 2001 IEEE GaAs Integrated Circuit Symposium.

Mohamed I. Elmasry (S'69–M'73–SM'79–F'88) was born in Cairo, Egypt, in 1943. He received the B.Sc. degree from Cairo University, Cairo, Egypt, and the M.A.Sc. and Ph.D. degrees from the University of Ottawa, Ottawa, ON, Canada, in 1965, 1970, and 1974, respectively, all in electrical engineering.

He has worked in the area of digital integrated circuits and system design for the last 40 years. He was with Cairo University from 1965 to 1968, and with Bell-Northern Research, Ottawa, ON, Canada, from 1972 to 1974. He has been with the Department of Electrical and Computer Engineering, University of Waterloo, Waterloo, ON, Canada, since 1974, where he is a Professor and Founding Director of the VLSI Research Group, also holding the University Research Fellowship, and was the National Sciences and Engineering Research Council of Canada/Bell Northern Research (NSERC/BNR) Research Chair in very-large-scale-integration (VLSI) design from 1986 to 1991. He has served as a consultant to research laboratories in Canada, Japan, and the United States. He has authored and coauthored more than 400 papers and 16 books on integrated circuit design and design automation. He holds several patents. He is the founding President of Pico Electronics, Inc., Waterloo, ON, Canada.

Dr. Elmasry has served in many professional organizations in different positions and received many Canadian and International awards. He is a Founding Member of the Canadian Conference on VLSI, the Canadian Microelectronics Corporation, the International Conference on Microelectronics, the Canadian Research Centers of Excellence, MICRONET, and CITO. He is a Fellow of the Royal Society of Canada and of the Canadian Academy of Engineers.